buildings

MDPI

Review

Research Progress on Shear Characteristics and Rapid Post-Disaster Construction of Narrow-Width Steel Box–UHPC Composite Beams

Yunteng Chen [1,2], Jiawei Xu [3,*], Peilong Yuan [3,4], Qiang Wang [4], Guanhua Cui [3] and Xulin Su [3]

[1] School of Civil Engineering, Shaoxing University, Shaoxing 312000, China
[2] Shaoxing Communications Investment Group Co., Ltd., Shaoxing 312000, China
[3] School of Highway, Chang'an University, Xi'an 710064, China
[4] CCCC Second Highway Engineering Co., Ltd., Xi'an 710075, China
* Correspondence: jiaweixu@chd.edu.cn

Abstract: The narrow-width steel box girder is an important type of steel–concrete composite bridge structure, which is usually composed of reinforced concrete wing plates, narrow steel boxes partially injected with concrete, and shear connectors that promote shear force transfer. The utilization of narrow-width steel box girders, augmented by partially filled concrete, embodies the synthesis of steel and concrete elements, fostering structural efficiency. Moreover, its attributes, including reduced structural weight, diminished vertical profile, enhanced load-bearing capacity, and augmented stiffness, have prompted its gradual integration into bridge engineering applications. In this study, the calculated values of shear strength under three current design codes were reviewed, and the shear failure phenomena and its determinants of narrow-width steel box–ultra-high-performance concrete (UHPC) composite beams under negative bending moment conditions were investigated, which were mainly determined by shear span ratio, concrete wing plate, UHPC steel fiber content, UHPC plate thickness, and transverse partition inside the box. Concurrently, this paper evaluates two innovative structural designs, including a double-narrow steel box girder and a three-narrow steel box girder. In addition, strategies to reduce crack formation under the negative bending moment of long-span continuous narrow and wide box girder abutments are discussed, and we show that this measure can effectively control the formation of cracks to support the negative bending moment zone. At the same time, the scope of the application of a narrow-width steel box girder composite bridge is reviewed, and the conclusion is that a narrow-width steel box girder is mainly used in small-radius flat-curved bridges or widened-ramp bridges with a span of 30 m or more in interworking areas and in the main line with a 60–100 m span in mountainous or urban areas. Finally, the research direction of the shear resistance of the UHPC–narrow steel box girder under negative bending moments is proposed.

Keywords: narrow steel box girder; negative moment zone; shear capacity; rapid construction

check for updates

Citation: Chen, Y.; Xu, J.; Yuan, P.; Wang, Q.; Cui, G.; Su, X. Research Progress on Shear Characteristics and Rapid Post-Disaster Construction of Narrow-Width Steel Box–UHPC Composite Beams. *Buildings* **2024**, *14*, 1930. https://doi.org/10.3390/buildings14071930

Academic Editor: Mizan Ahmed

Received: 28 April 2024
Revised: 17 June 2024
Accepted: 18 June 2024
Published: 25 June 2024

Copyright: © 2024 by the authors. Licensee MDPI, Basel, Switzerland. This article is an open access article distributed under the terms and conditions of the Creative Commons Attribution (CC BY) license (https://creativecommons.org/licenses/by/4.0/).

1. Introduction

As economic development advances, the demand for infrastructure construction in China is experiencing steady growth. With the continuous development of bridge construction, the number of bridges in mountainous areas is increasing day by day [1], and the rapid development of bridges after a disaster has become an important research topic. Taking the mountainous area of Sichuan, China as an example, the region is prone to frequent geological disasters, such as debris flow and earthquakes [2]. The necessity of the rapid reconstruction of bridges after a disaster is reflected in the following aspects: providing temporary shelter and infrastructure, restoring social order and economic activities, reducing the long-term impact of disasters, and improving the efficiency of emergency rescue are important links in post-disaster reconstruction. Concurrently, the advancement of high-

way engineering is paralleled by ongoing progress and development in the construction techniques and theoretical frameworks of bridges and tunnels [3–26].

Composite system that integrates the strengths of both steel and concrete structures [27]. Steel–concrete composite structures offer the advantage of reducing the amount of steel required for construction compared to conventional steel structures [28]. They enhance structural stiffness, durability, stability, and fire and shock resistance [29]. This approach utilizes steel beam-laminated concrete bridge panels to maximize the exceptional tensile properties of steel and the favorable compressive properties of concrete. Amidst the ongoing evolution of various steel–concrete composite beams, a novel structure has arisen: narrow steel box–concrete composite beams, depicted in Figure 1. Its main features are that the main bearing steel beam is designed into a narrow box shape, the width of the box does not exceed 1/2 of its height, and the box is connected by a beam and then superimposed to a concrete bridge panel. Figure 1 briefly illustrates the difference between the narrow steel box girder structure and the ordinary steel box structure. In the follow-up study on the influence of the width/height ratio of the box girder on the performance of the composite beam bridge, it is necessary to reduce the thickness and ensure that the filling amount of concrete is equal.

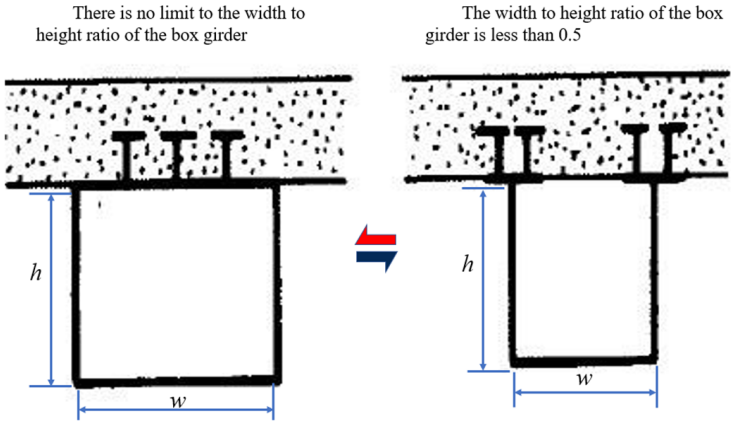

Figure 1. Comparison between concrete composite beams and narrow steel box beams.

Compared to other bridge types, narrow steel box–concrete composite bridges offer advantages such as reduced construction costs, low construction complexity, and shorter construction durations, as shown in Figure 2. This type of bridge is particularly well-suited for environmental conditions, such as mountainous terrains, where traditional construction methods may be challenging. Additionally, it holds the potential for widespread adoption and applications in the reconstruction of highways that have been severely impacted by earthquake disasters. Steel–concrete composite beam bridges offer unique advantages in mountain road construction, particularly in the aftermath of disrupted traffic conditions following an earthquake: (1) Compared to concrete structure bridges, the weight of the bridge span is significantly reduced. The steel beams utilize a separate body combination method, resulting in lightweight unit components that facilitate factory prefabrication and transportation in mountainous regions. (2) The bridge can be rapidly erected and constructed without the need for large lifting equipment. During construction, workers do not have to work in the steep gullies and riverbeds that are common in mountainous regions, leading to significant savings in support materials and labor [30]. The prefabrication of steel box girders and bridge panels can proceed concurrently with the construction of the substructure without being constrained by time or location. (3) Once the bridge pier is constructed, the installation and construction of the bridge span can proceed as usual, even during periods of flooding [31]. (4) The steel–concrete composite beam bridge makes full use of the advantages of steel and concrete, and through reasonable structural design, it can minimize the use of materials while ensuring the strength and bearing capacity, thus reducing the material cost. Compared to the traditional pure steel bridge or pure concrete

bridge, the construction period of the steel–concrete composite beam bridge is relatively short. Due to the use of prefabricated components and the process of on-site assembly, the construction period can be greatly shortened, the usage time of labor and equipment can be reduced, and the construction cost can be reduced. Thanks to the aforementioned advantages of narrow-width steel box girders, they have increasingly been utilized in the rapid reconstruction efforts following earthquakes and in construction projects undertaken in challenging geographical environments, particularly in mountainous areas. The spacing between the two main I-beams of the Hospital Bridge [32] completed in France in 1990 is 12.6 m, indicating that the spacing between steel boxes can further expand the application range of the double-narrow steel box. The simple configuration of double main beams is clearly desired in both the design and construction phases. Structural analysis revealed that the structural system of a double main beam bridge, featuring a steel main beam roof with large-section stiffness and a concrete bridge panel, forms a composite structure.

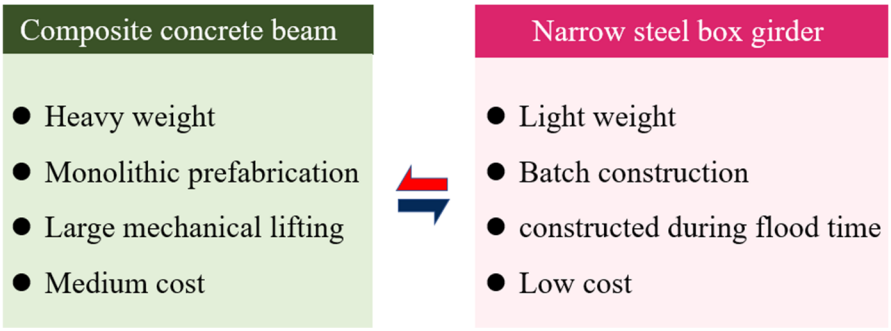

Figure 2. Advantages of the post-disaster reconstruction of the narrow-width steel box girder.

The economic span-to-height ratio of steel–concrete composite beams typically ranges from 1/20 to 1/18 [33]. This value can be further reduced with the introduction of external prestressing. The thickness of the steel box web, top, and bottom plates should be determined by considering factors such as steel strength, box height, and the presence of stiffening ribs in a comprehensive manner. Without stiffeners, the thickness of the steel plate should generally be at least 1/150 of the beam height. Longitudinal and transverse stiffeners can be added to the steel box as needed.

The introduction of narrow-width steel box girders offers a new structural option for concrete composite beam bridge systems. However, there is ongoing development in the design improvement of narrow-width steel box girders. Within the composite continuous beam system, the negative bending moment tends to concentrate close to the cross-section of the central support [34] and the conventional steel–concrete composite section of the concrete wing exhibits signs of separation and fracturing [35]. It fails to effectively fulfill its role in withstanding external forces, with the steel beam predominantly situated within the compression zone of the section, leading to overall stability concerns. Consequently, a densely packed narrow steel box–concrete composite continuous beam, illustrated in Figure 3, is proposed. This configuration typically comprises reinforced concrete wing plates, narrow steel boxes partially filled with concrete, and shear connectors facilitating shear force transmission. The densely packed narrow steel box–concrete composite continuous beam constitutes the interconnection of the concrete wing plate and the concrete-filled steel box beam via shear connectors [36]; given that the steel box adjacent to the side support, middle support, and negative moment region experiences significant shear forces, it may be infused with concrete to augment the coaction between the steel box and enhance the flexural and shear strength within this segment. The concrete wing slab in the negative moment zone of the densely packed narrow steel box and the concrete composite continuous beam are subjected to tensile forces. In the case of the NC (ordinary concrete) wing slab in the negative moment zone, it is suboptimal to postpone the initiation of initial cracking [37], while the concrete wing slab of the composite beam retains an ideal reserve of

strength and stiffness after cracking; it is imperative to mitigate the accelerated corrosion of steel bars following cracking [38]. Minimizing crack propagation in the negative moment zone during normal usage is imperative. Moreover, the swift advancement of research on ultra-high-performance concrete (UHPC) has captivated the interest of numerous scholars owing to its exceptional mechanical properties. Mo [37] pioneered the utilization of UHPC wing plates, replacing conventional NC (ordinary concrete) wing plates, in the negative moment region of composite beams. This innovative approach effectively addressed the issue of cracking observed in narrow steel box girder wing plate concrete.

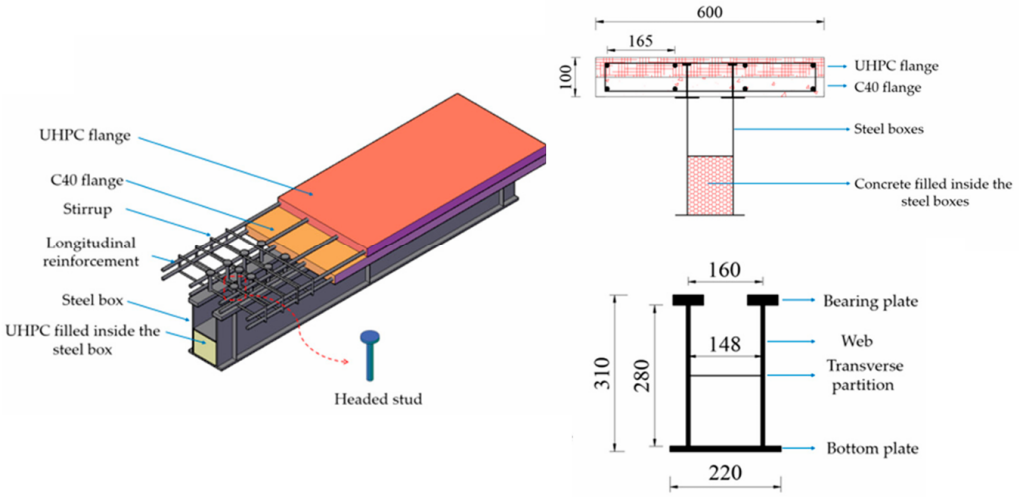

Figure 3. UHPC wing plane–narrow steel box continuous beam structure [35].

In recent years, research on the performance of ultra-high-performance concrete (UHPC) in composite beam structures has significantly advanced. Tadesse G. Wakjira et al. [39] employed the Conditional Form Generation Adjunct Network (CTGAN) and the Optuna-enhanced machine learning (ML) model to predict the stress–strain response of unconfined UHPC, accurately forecasting peak and ultimate axial stress–strain responses under different steel constraints. Roya Solhmirzaei et al. [40] proposed a data-driven ML framework to predict UHPC beam failure patterns and shear resistance, using algorithms like the support vector machine (SVM), artificial neural network (ANN), K-nearest neighbor (k-NN), and genetic programming (GP) to identify key parameters. Wakjira et al. [41] also developed a stress–strain constitutive model for UHPC using mixed ML techniques, which accurately predicts the confined UHPC stress–strain response.

The advancement of ML technology has greatly contributed to UHPC constitutive model research, aiding the design and application of narrow steel box–UHPC composite beam structures, especially in earthquake-prone mountainous areas. Despite UHPC's high performance, its initial cost can be prohibitive.

However, UHPC production can be costly due to high-cost materials like silica fume and superplasticizers, along with a substantial amount of cement. Using supplementary cementitious materials such as slag and fly ash, which are readily available, it is possible to reduce UHPC material costs. Notably, fly ash availability in North America has declined due to stricter environmental regulations on coal combustion for energy production. Furthermore, UHPC production has significant environmental impacts, necessitating a comprehensive evaluation of its overall environmental footprint. Therefore, optimizing UHPC mixtures for cost and sustainability is crucial. Wakjira et al. [42] created a reliable uniaxial compressive strength prediction model by combining tree and boost integration ML models, considering 19 objective functions, including cost and various environmental impact categories. This study offers valuable tools for designers to select optimal UHPC mixes for specific engineering needs. Reducing UHPC costs, considering sustainability

indices, and optimizing mixtures under varying design requirements remain important research topics.

Numerous studies have been conducted to investigate the mechanical properties and influential parameters of steel–concrete composite structures [38–45]. Ensuring the optimal mechanical performance and durability of composite beams while operating under cracked conditions has emerged as a key research focus for numerous scholars. The predominant focus of the current research lies on steel beams featuring T-shaped or I-shaped sections [36,43,45]. Furthermore, limited research has been conducted on the interface of narrow steel box beams. In this study, we review the research progress and influencing factors related to the shear resistance in the negative moment zone of narrow-width steel box–UHPC composite beams. Additionally, we discuss the applicability and accuracy of various shear capacity codes and review the research progress on rapid construction methods following seismic events. Lastly, we present conclusions and suggestions for further research on the shear performance and rapid construction of UHPC–narrow-width steel box girders.

2. Overview of Shear Resistance Tests of Narrow-Width Steel Box–UHPC Composite Beams

2.1. Preparations for Experiments

The narrow-width steel box–UHPC composite beam primarily consists of a concrete wing plate and a steel box beam, connected through shear connectors and filled with ultra-high-performance concrete (UHPC) [46]. The production process of the narrow-width steel box–UHPC composite beam (NSBCB) structure entails several stages, including steel box fabrication, concrete filling within the box, steel mesh binding, wing mold preparation, and wing plate casting [47], as shown in Figure 4.

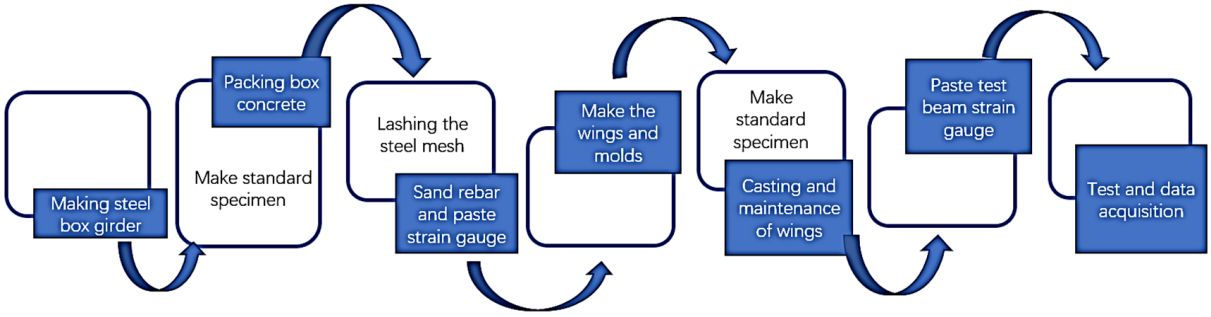

Figure 4. Specimen production process [47].

During the fabrication and welding of the steel box, flexible shear connectors, typically bolts, are used, and welding is initiated with a welding gun attached to the steel beam flange. High-strength steel plates are used to weld the steel box, and stiffeners are welded to the support area at the loading point. Liu et al. [48] found that infusing core concrete in the lower section of the negative moment zone creates a synergistic interaction between the materials, reducing compressive stress concentration and preventing inward buckling of the steel box girder.

After filling the box with concrete, a vibrator ensures uniform vibration of the core concrete. The steel box is then positioned horizontally for curing. To ensure the strength of the wing panels [49], material mixtures were strictly controlled to use the same batch of concrete. The concrete was quickly transported to the pouring platform and uniformly poured from the middle to both ends of the span. Delays in concrete preparation can cause bonding issues, reducing wing slab strength [50]. After 28 days of curing at room temperature, all specimens underwent tests for compressive strength, flexural strength, and splitting strength, as shown in Figure 5.

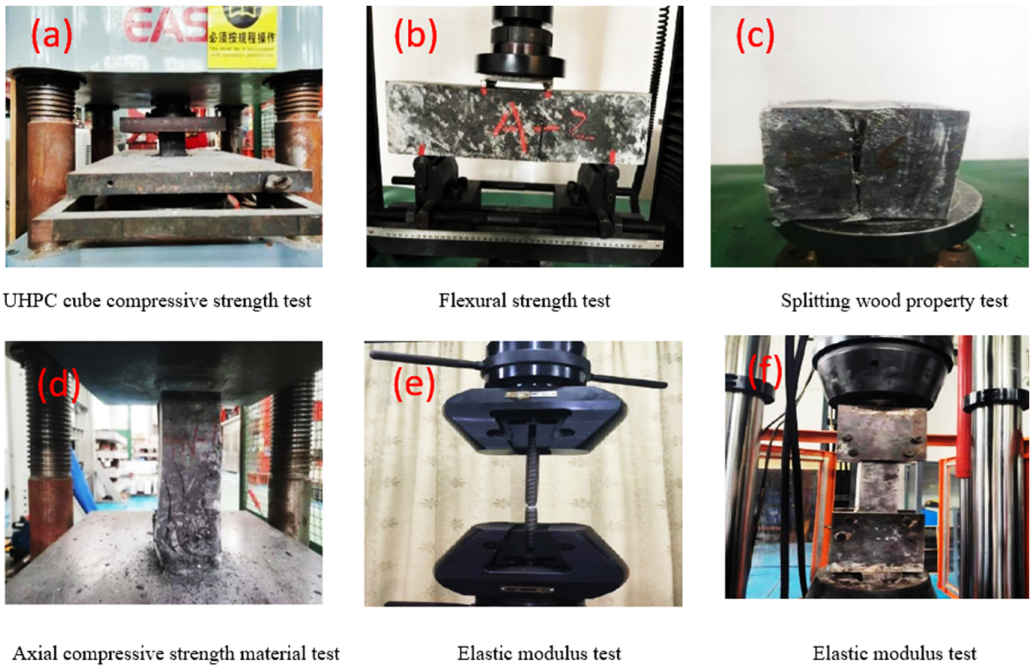

Figure 5. Material property test [50].

2.2. Experimental Tests

Prior to conducting the shear test on the narrow-width steel box–UHPC composite beam, it is essential to ascertain the strength and type of concrete employed. Concrete strength can be assessed through the examination of prepared specimens. According to He [51], augmenting the concrete strength can substantially enhance the stiffness, strength capacity, and bending moment capacity of narrow-width steel box–UHPC composite beams. The test primarily encompasses evaluations of interface slip between the wing plate and the steel beam, mid-span deflection, wing plate strain, steel beam strain, and wing plate crack propagation, among others [52].

A slip meter measures slip at the wing plate and steel box beam interface. Strain gauges measure strain distribution at various locations on the test beam. The locations include the mid-span steel box girder's web, the steel beam's web along its height, the main rib of the wing plate, the top surface of the wing span, and the mid-side of the span. A displacement meter is installed at the loading point and support position to generate the load–deflection curve [53]. Strain data are collected using a strain-collecting instrument, while displacement measurements are obtained manually. The crack distribution of the wing plate is monitored with a crack observation instrument during the test loading. Two common loading methods are used: three-point bending and four-point bending as shown in Figure 6. The four-point bending test (4PBT) is commonly used to assess shear behavior in the positive moment region, while the three-point bending method is typically used for shear tests on continuous beam bridges in practical engineering. However, some studies use the four-point bending method to comprehensively analyze the combined action of composite beam bridges [54].

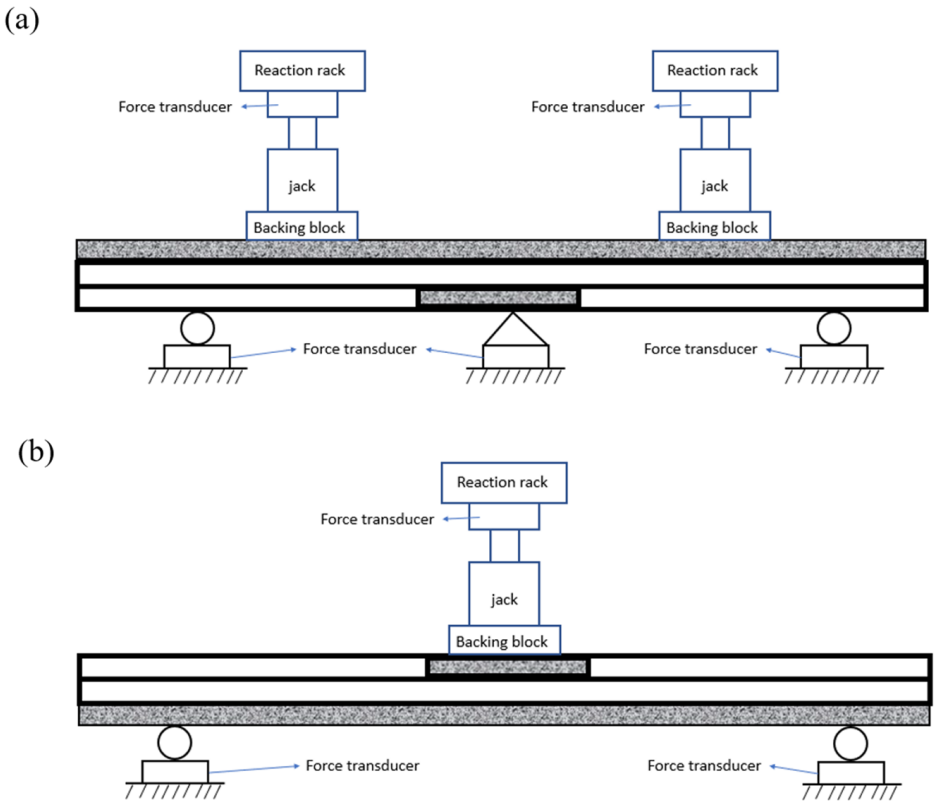

Figure 6. Loading mode and loading device (**a**) three-point bending (**b**) four-point bending [36].

2.3. Failure Modes

Steel–UHPC beams can fail in different ways based on loads, materials, and geometry. Maximum shear capacity is achieved when the wing plate and steel box fail simultaneously. Practical applications may experience overall failure due to single or multiple local failures. The literature review indicates that under negative bending moments, the failure of narrow-width steel box girder–UHPC composite beams is characterized by buckling deformation, cracks on the upper wing plate, and localized concrete crushing. The typical failure modes of narrow-width steel box girder–UHPC composite beams are summarized in Table 1. Mo et al. [37] reported that flexural shear failure occurred mainly due to shear action, and the mid-span of the wing plate was cracked by bending action. Due to the action of pegging, the lateral cracks on the wing plate developed slowly and appeared as steps between the UHPC–NC layers. The cracks in the upper part of the wing plate developed approximately equidistant from the stud spacing, which was due to the stress concentration caused by the local strengthening of the stud in the inner section of the wing plate. Shear oblique cracks appeared on the side of the wing plate at the support, accompanied by the slip between the UHPC–NC wings. The steel beam buckled at the loading point and the middle partition. Liu et al. [34] reported that the main fracture across the flange was observed on the fragile surface located at the midpoint of the test beam, and the final failure mechanism observed in the six test beams was remarkably similar. When the steel wire in UHPC was extracted, the delamination between the flange and the steel bar was observed at the crack location. Due to the relative displacement, longitudinal cracks and delamination appeared between the UHPC layer and the C40 layer of the flange, and diagonal cracks appeared on the side of the flange. In general, the test beams exhibited typical tensile fracture characteristics, such as local buckling and observable shear deformation in the lower part of the steel box girder. Xiong et al. [47] reported that filling concrete inside the steel box of UHPC composite beams can significantly improve the shear resistance of the specimens. When the steel box was not filled with concrete, the bending deformation of the box beams resulted in brittle failure of the test beams, while the other test beams had similar mechanical characteristics, resulting

in bending and shear failure mainly caused by shear action; the wing plates were cracked by bending action in the middle span. According to the literature review, the main failure of the UHPC composite beam under the condition of negative moment zone is buckling deformation of the box girder, surface crack of the wing plate, and local concrete crushing, as shown in Figure 7.

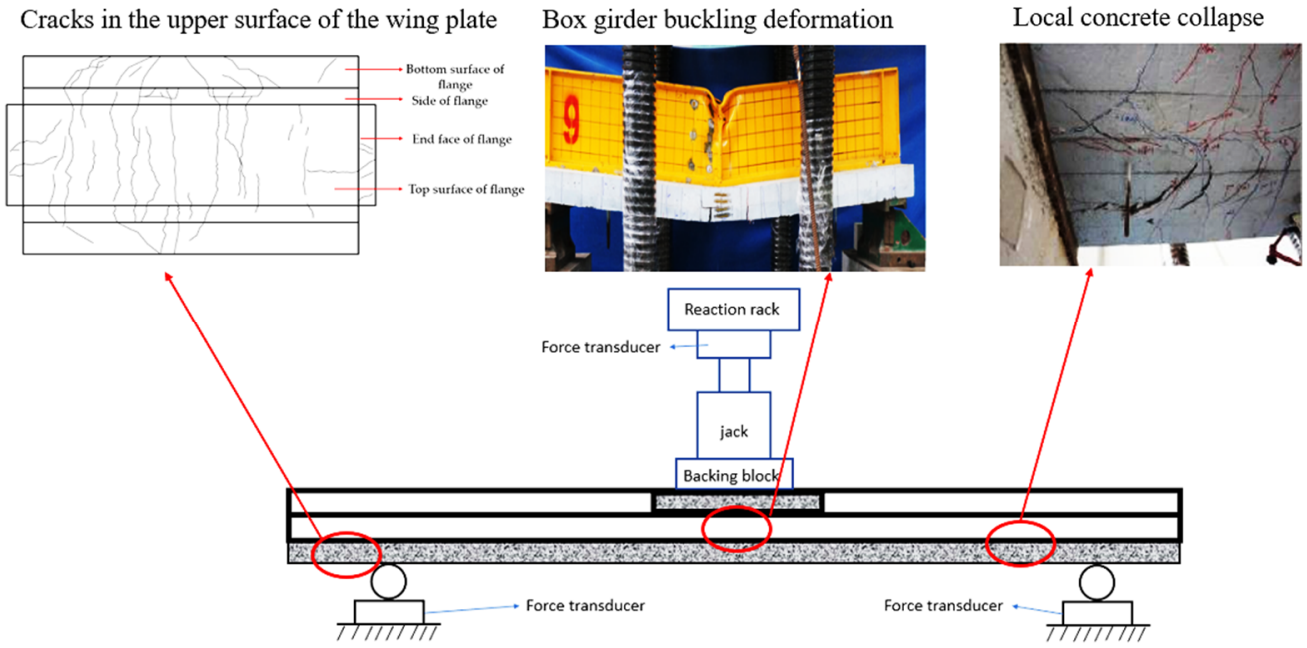

Figure 7. Typical failure mode [47].

Simultaneously, through a literature review of load–span deflection [27,34,36,37,43,47–49,51–57], we can roughly categorize the deflection curve into three stages.

(1) Elastic stage (V < Vy)

A linear relationship exists between the stage load and deflection, and the steel beam remains unyielding. However, under the negative bending moment, a few cracks emerged, and the composite beam wing showed some plastic deformation.

(2) Elastoplastic stage (Vy < V < VU)

As the load increases, the crack width of the primary crack in the middle span of the wing plate accelerates, leading to partial yielding of the steel bar and internal force redistribution within the section. Consequently, the proportion of plastic deformation in the beam increases, resulting in decreased stiffness, amplified deflection of the wing plate, and nonlinear deflection progression with increasing load. This signifies the onset of the failure stage.

(3) Plastic stage

As the bridge structure is further loaded, it enters the complete shaping stage. The full shaping stage is usually short as the deflection increases. Once in the full shaping stage, the bridge structure quickly reaches its ultimate load, and the load decreases as the deflection continues to increase beyond the ultimate load.

(4) Failure stage

Upon reaching the ultimate load, the test beam transitions into the failure stage. As the deflection of the test beam increases, the load diminishes to some extent, accompanied by the widening of the main crack. Subsequently, the steel box web plate exhibits baroclinic buckling, while the bottom plate of the steel beam bulges at the point of the concentrated force application. This leads to a sharp increase in deflection and a rapid reduction in the

bearing capacity due to shear failure. Figure 8 illustrates the load–mid-span deflection curves of six specimen beams under various parameter conditions as reported by Liu et al. It is observed that upon entering the plastic stage, the stiffness of the UHPC composite beam notably decreases, with cracks appearing on the upper surface of the wing plate upon further loading (Figure 9). After entering the failure stage, the steel beam experiences partial buckling deformation (Figure 9), eventually rendering it incapable of fulfilling its intended function.

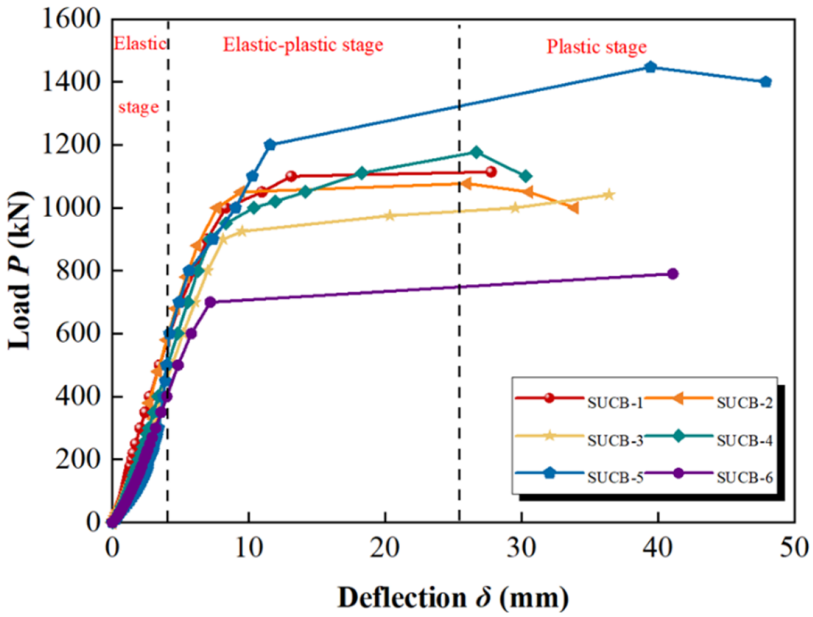

Figure 8. Load–mid-span deflection curve [34].



Figure 9. Failure characteristic [47].

Table 1. Typical shear failure mode of the UHPC composite beam.

References	Box Girder Concrete Filling Height/Box Girder Height	Box Girder Concrete Strength (MPa)	UHPC Wing/Wing Thickness	Loading Protocol	Comments	Typical Failure Mode
Xiong et al. [47]	0.5	38.54	0 0.5 1	Force control is used throughout. The formal loading starts at 0. Before the concrete wing cracks, the load of each stage is 10 kN after the cracking, and the load is adjusted to 50 kN. After the load is loaded, the load step is adjusted to 100 kN per stage when the load-displacement curve of the composite beam is no longer linear.	The failure characteristics include the diagonal buckling of the steel beam web and the loss of bearing capacity of the UHPC wing plate due to the pulling out of the steel fiber.	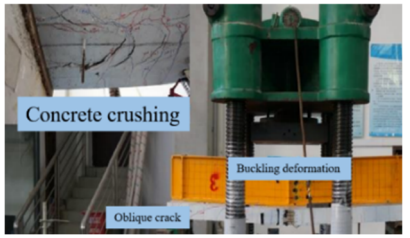
Wang et al. [55]	0.5	45	0	The loading method of each stage is hierarchical, and the corresponding loading size of each stage is selected according to the observation requirements.	The failure stage of the test beam can be divided into the elastic stage, shaping stage, and failure stage.	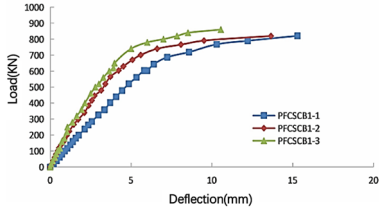
Liu et al. [34]	0.5	42	0.5	In the elastic stage, the force-controlled loading technique is used to increase the load by 10 kN per layer. After the transition to the elastoplastic stage, the load increment of each layer is increased by 50 kN.	The deflection at the middle point of the steel box girder increases the fastest, and the bottom plate and web plate of the steel box girder produce buckling deformation.	

Table 1. *Cont.*

References	Box Girder Concrete Filling Height/Box Girder Height	Box Girder Concrete Strength (MPa)	UHPC Wing/Wing Thickness	Loading Protocol	Comments	Typical Failure Mode
Zhang et al. [56]	1	58	0	Force control	The load drops sharply after Vu, indicating brittle failure of the tested beam. During the whole loading process, the mid-span top concrete of all the beams was not crushed.	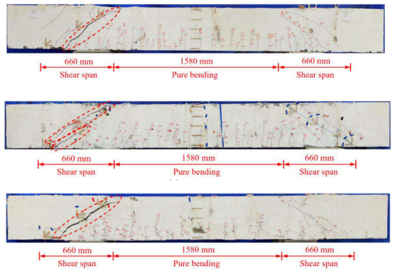
Mo et al. [37]	0.5	38.5	0 0.5 1	Loading protocol	Comments	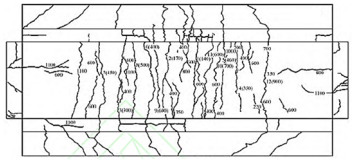

3. Review of the Shear Code Guidelines and Analysis of the Influencing Factors in the Negative Moment Zone of the Narrow-Width Steel Box–UHPC Composite Beam

3.1. Specification Guidelines for Shear Resistance in the Negative Moment Zone

To confirm the applicability of different design codes to the evaluation of the shear resistance of steel box–UHPC composite beams, we reviewed and analyzed the calculated values of three codes that are mainly used in the world today. These specifications will be used later in the shear behavior analysis.

(1) American AASHTO specification [58]

The American AASHTO bridge design code stipulates that only the contribution of composite steel beams is considered in the shear design, and the shear capacity of concrete bridge panels is ignored. Under the action of the negative bending moment, the calculation formula for composite beams with stiffened webs is as follows.

$$V_{cr} = V_p \left[C + \frac{0.07(1-C)}{\sqrt{1+(d_0+D)^2}} \right]$$

$$\frac{2D_t}{b_{fc}t_{fc} + b_n t_{ft}} \le 2.5n$$

$$V_p = 0.58 \times 10^{-3} F_{yw} D_{tw},$$

$$C = \begin{cases} 1.0, & \frac{D}{t_w} \le 1.12\sqrt{\frac{E_K}{F_{yw}}} \\ \frac{1.12}{D/t_w}\sqrt{\frac{E_k}{F_{yw}}}, 1.12\sqrt{\frac{E_K}{F_{yw}}} \le \frac{D}{t_w} \le 1.4\frac{E_K}{F_{yw}} & \\ \frac{1.57E_K}{\left(\frac{D}{t_w}\right)^2 F_{yw}}, D/t_w & > 1.4\frac{E_K}{F_{yw}} \end{cases}$$

where V_{cr} is the buckling capacity of the steel beam web, C is the ratio of the shear buckling capacity to the plastic shear capacity of the steel beam web, V_p is the plastic shear strength of the steel beam web, F_{yw} is the buckling strength of the steel beam web, D is the height of the steel beam web, t_w is the thickness of steel beam web, b_f is the height of the steel beam compression roof, t_{fc} is the thickness of the compression roof of the steel beam, tft is the thickness of the tensile roof of the steel beam, d0 is stiffener spacing for the web, and k is the shear buckling coefficient, which is set to 5 when there is no stiffener.

(2) European specification EC4 [59]

The formula for calculating the shear strength of EC4 steel-mixed composite beams considers the effect of buckling on shear performance by introducing a partial coefficient, i.e., γ_{Rd}, for local web plate buckling, with a value of 1.1. The vertical shear capacity of the steel-mixed composite beams is then determined by the formula V_b, R_d.

$$V_{b,Rd} = \frac{\tau_{ba} A_v}{\gamma_{Rd}}$$

Among them, the shear strength of the steel beam, i.e., τ_{ba}, will change with the change in the web length ratio, i.e., λ_w, after buckling.

$$\tau_{ba} = \begin{cases} \frac{0.9f_y}{\overline{\lambda_w}\sqrt{3}}, \overline{\lambda_\omega} \ge 1.2 \\ \left[1 - 0.625\left(\overline{\lambda_w} - 0.8\right)\right]\frac{f_y}{\sqrt{3}}, 0.8 < \overline{\lambda_w} < 1.2 \\ \frac{f_y}{\sqrt{3}}, \overline{\lambda_w} < 0.8 \end{cases}$$

(3) Chinese Code for the Design of Steel–Concrete Composite Bridges [60]

When calculating the vertical shear capacity of composite beams, the current industry standard GB 50917-2013 [60] stipulates that only the contribution of the steel girder web to

composite beams is considered, and the ultimate vertical shear capacity is calculated using the plastic limit design method.

$$\gamma_0 V \leq h_w t_w f_{vd} \times 10^{-3}$$

where γ_0 is the structural importance coefficient, V is the design value of the shear force of the composite beam, h_w is the effective height of the steel beam web, tw is the thickness of the steel beam web, and f_{vd} is the design value of the shear strength of the steel beam web.

3.2. Examination of the Experimental Results of the Narrow-Width Steel Box–UHPC Composite Beam

European and American codes for composite beams account for buckling and plastic deformation of steel beam webs, while the Chinese code only considers the plastic shear contribution and ignores local buckling effects. Consequently, the Chinese code adopts a conservative approach. A comparison shows that U.S. norms yield the highest shear capacities, while China's are the lowest, primarily due to conservative steel strength values.

The Table 2 shows that only considering the contribution of the web to the shear strength will make the calculated value of the shear strength much smaller. Among them, the calculated value provided by GB 50917-2013 is the most conservative, and the average value of the calculated value to the test value (v_c/v_t) is about 0.65, while the value (v_c/v_t) obtained by the American AASHTO specification is the largest. However, it is not difficult to observe that regardless of the above three specifications, the predicted shear strength obtained is less than 70% of the actual shear strength, which will lead to a great waste of design strength in the actual design process. At the same time, to obtain the shear strength to meet the design requirements, the box height of the composite beam will be increased, and the proportion of the bridge's self-weight load will be greatly increased, which is unfavorable to the bearing capacity of the composite beam. Therefore, it is necessary to study the calculation theory of shear strength, which is closer to practice.

Table 2. Comparison of the test values to those calculated by national norms.

ID	Test Value of Shear Capacity	American Calculated Value	Ratio	European Calculation	Ratio	Chinese Calculated Value	Ratio
1 [47]	625	312	0.4992	308	0.4928	299	0.4784
	600	312	0.52	308	0.513333	299	0.498333
	550	312	0.567273	308	0.56	299	0.543636
	650	312	0.48	308	0.473846	299	0.46
	700	312	0.445714	308	0.44	299	0.427143
	395	312	0.789873	308	0.779747	299	0.756962
2 [48]	315	312	0.990476	308	0.977778	299	0.949206
	341	312	0.914956	308	0.903226	299	0.876833
	376	312	0.829787	308	0.819149	299	0.795213
	304	312	1.026316	308	1.013158	299	0.983553
	393	312	0.793893	308	0.783715	299	0.760814
	393	312	0.793893	308	0.783715	299	0.760814
3 [54]	557	312	0.560144	308	0.552962	299	0.536804
	538.5	312	0.579387	308	0.571959	299	0.555246
	520	312	0.6	308	0.592308	299	0.575
	588.5	312	0.530161	308	0.523364	299	0.508071
	723.5	312	0.431237	308	0.425708	299	0.413269
	395	312	0.789873	308	0.779747	299	0.756962
Mean value			0.674566		0.665918		0.646459

A review of UHPC–NC composite beams and experimental studies reveals the crucial role of the wing plate in shear strength. Therefore, the shear capacity of each part should be considered and summed to obtain the total shear capacity. As Pu Zhang [56] reported, the shear carrying capacity of the UHPC–NC beam was divided into three parts, i.e., V_{NC} provided by the NC part, VUHPC provided by the UHPC formwork, and Vsg provided by the steel grid. Luaay Hussein [61] reported that the shear resistance of a UHPFRC-NSC/HSC beam is thus equivalent to the expected shear resistance of an NSC/HSC beam without shear reinforcement, i.e., V_c, plus the additional shear resistance provided by the fibers, i.e., V_f, due to the improved post-cracking resistance of the UHPFRC layer. The shear strength of UHPFRC-NSC/HSC composite beams can be calculated from $V_u = V_c + V_f$. Using the principle of partial superposition proposed by Shuai Liu [34], we formulated an equation for the numerical assessment of the influence of concrete filling on shear capacity. Men Pengfei [62] reported that it is necessary to comprehensively consider the influence of the section form of the wings and the tensile strength of concrete on the shear capacity of composite beams and proposed a calculation method for the shear capacity of the wings considering the buckling form of the web of steel beams:

$$V_{fuc} = \alpha_1 f_{tk} b_c h_c + \alpha_2 \rho f_{tk} b_c h_c = (\alpha_1 + \alpha_2 \rho) f_{tk} b_c h_c$$

Leveraging the principle of superposition calculation of the shear capacity for each component, numerous scholars have conducted additional investigations into the shear force calculation formula for narrow-width steel box girders. Nonetheless, a comprehensive and universally applicable calculation criterion remains elusive for narrow-width steel box girders. Hence, further review and study of the calculation formula for the shear capacity of narrow-width steel box girders are imperative.

3.3. Analysis of the Influencing Factors on the Shear Strength of the Narrow-Width Steel Box–UHPC Composite Beam

Similar to the traditional steel–concrete composite beam bridge structure, the factors affecting the shear resistance of narrow-width steel box–UHPC composite beams can be divided into geometric factors and material factors. Among them, a considerable number of the factors are the same as the narrow steel box girder and the concrete composite beam bridge (as shown in Figure 10), such as the shear span ratio, the strength of concrete and steel materials, and so on. Therefore, in this section, we focus on the unique factors affecting the shear strength of narrow-width steel box–UHPC composite beams (shown by the star in Figure 10).

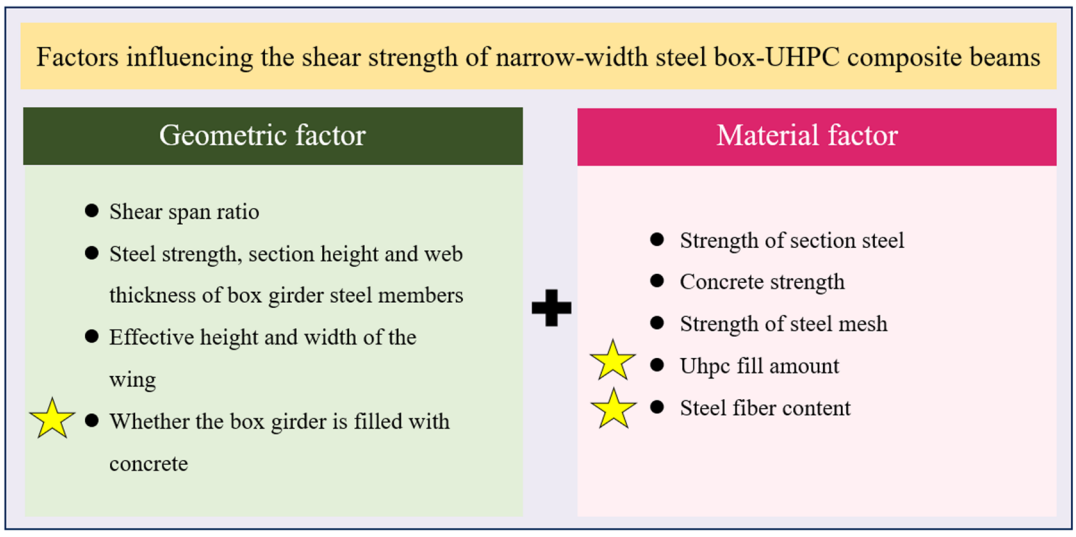

Figure 10. Influencing factors of shear resistance.

(1) Shear span ratio

The generalized shear span ratio of composite beam concrete panels closely resembles that of ordinary reinforced concrete beams. Research findings [46] indicate that for shear span ratios below 4, shear strength exhibits an inverse correlation with the shear span ratio.

(2) Steel box girder

The steel section of the composite beam significantly influences its shear strength. With all other factors held constant, increases in steel strength, section height, and web thickness correspondingly enhance the shear strength of the composite beam. In practical scenarios where the overall shear strength of the composite beam falls short of standards, adjustments typically involve augmenting the web thickness and elevating the section height of the steel beam.

(3) Concrete wing slab

The strength of concrete material also affects the shear strength of composite beams, albeit to a lesser extent than steel beams. Enhancing the effective height and width of the wings can marginally enhance shear strength. Additionally, incorporating steel mesh within the concrete slab augments the shear strength and stiffness of the composite beam. While the primary compressive stress in the concrete wing slab is borne by the steel mesh under positive bending moments, its impact on shear strength is minimal. Conversely, under negative bending moments, the concrete wing slab experiences predominantly tensile stresses, posing unfavorable conditions. However, the steel mesh effectively mitigates concrete slab cracking, thereby enhancing the cross-section stiffness and overall shear-bearing capacity of the composite beam [34]. When cracks were initiated within the flange, the steel fibers embedded in the UHPC material with diverse orientations exhibited a 'bridging effect', effectively mitigating the propagation of cracks.

In addition to the above factors, UHPC steel fiber content, UHPC board thickness, and filled concrete have a great influence on the narrow steel box–UHPC composite beam in the negative bending moment area. Through the review of the literature [36,46,54,55,59,61–65], we compiled a database of the test results, as shown in Table 2, and collected the detailed shear test data of narrow-width steel box–UHPC composite beams from 11 typical articles, as shown in Tables 1 and 2. Through a review of the above literature, we obtained the key influencing factors of narrow-width steel box–UHPC composite beams.

(1) UHPC steel fiber content

Introducing steel fibers effectively curtails wing plate cracking, leading to the development of numerous narrow and dense cracks upon failure. This demonstrates that the inclusion of steel fibers in UHPC enhances the shear strength of composite beams to a certain extent while substantially enhancing their ductility.

When the steel fiber content of UHPC changes [29], the steel fiber content increases from 0 to 2%, and the ultimate loads of the composite beams are 1300 and 1250 kN, respectively, with a difference of only 4%, as shown in Figure 11a. The steel fiber content has little effect on the bearing capacity of the composite beams. However, during the crack development of the specimen, it can be observed that the crack development speed of the test beam decreases after the addition of steel fibers. When the maximum crack width is 0.2 mm, the loads of the specimens SUCB-1 (steel fiber content of 2%) and SUCB-2 (without steel fiber addition) are 500 and 330 kN, respectively. Adding steel fibers can effectively improve the cracking resistance of composite beams.

(2) UHPC board thickness

As the composite beam is subjected to shear action mainly under the action of the negative bending moment, the concrete wing slab of the composite beam will suffer shear failure. According to the test results, when the other parameters remain unchanged and the thickness of the UHPC wing slab changes, compared to SUCB-3, the bearing capacity of SUCB-1 and SUCB-4 increased by 18.2% and 27.3% respectively, and the deformation

capacity increased by 38.02% and 41.2% respectively, as shown in Figure 11b. The increase in the thickness of UHPC fins can effectively improve the mechanical properties of composite beam fins and significantly enhance the shear-bearing capacity and deformation resistance of composite beams [29].

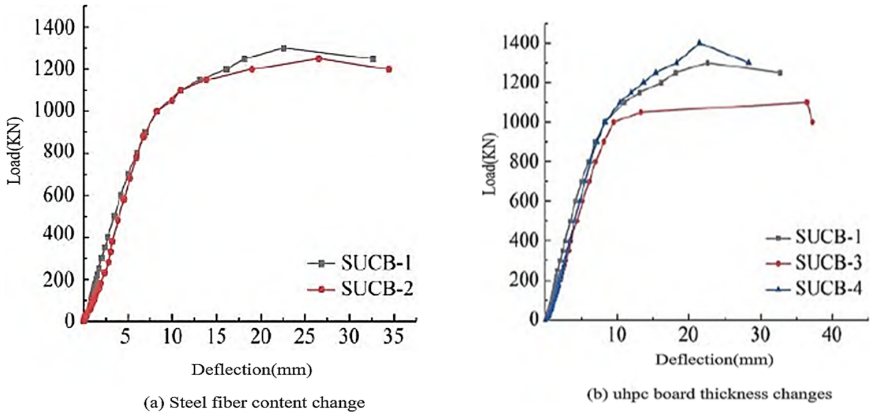

Figure 11. Influence of UHPC steel fiber content and UHPC plate thickness on shear strength [29].

(3) Filling concrete

Filling the narrow steel box with concrete improves the rigidity and stability of the composite beam and makes up for the lack of overall stability of the composite beam caused by reducing the effective width of the steel box. The load–deflection curve presents an upward trend with the increase in the UHPC height. By comparing the stiffness of composite beams at the initial loading stage, it is found that the stiffness of composite beams without UHPC filling inside steel beams is lower than that of composite beams with UHPC filling inside steel beams, as shown in Figure 12. In addition, the deformation ability of composite beams with half-filled UHPC narrow steel boxes is much greater than that of composite beams with full and unfilled narrow steel boxes. Filling UHPC inside steel boxes can not only improve the shear strength of composite beams but also enhance the deformation ability of composite beams. However, overall, half-filled UHPC narrow-width steel box composite beams are the best [43].

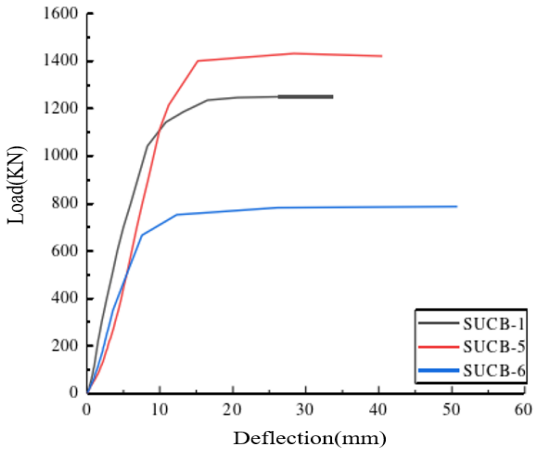

Figure 12. Effect of filling concrete on shear strength.

(4) Transverse partition in the box

The function of the transverse partition in the box is to prevent excessive deformation of the section, improve the torsion resistance of the section, and transfer the additional stress of the crossbeam between the boxes. According to the design guidelines of Japanese

Highway Steel Bridges [63], the spacing of the partitions in the bridge box is not more than 6 m. When the solid belly diaphragm is set, according to previous engineering experience and calculations, the stiffness of the diaphragm is relatively large, and the stress is generally not controlled by the design; so, the plate thickness of the cross-span diaphragm can be about 12 mm, and the fulcrum diaphragm generally needs to be thickened, which needs to be determined according to the checking calculation.

(5) Crossbeam between boxes

The function of the tinderbox beam is to maintain the structure shape during erection, reduce the relative deflection difference between the main beams, transfer the transverse load, reduce the stress of the single main beam through the transverse load distribution, and improve the torsional stiffness of the whole bridge. Because the steel–concrete composite beam is equipped with a strong concrete roof, the transverse load transfer and transverse load distribution effect of the beam are greatly reduced after erection.

(6) Shear connector

The shear connector plays a key role in combining the steel main beam and the bridge panel to work together [36]. According to existing engineering practice, stud connectors are flexible connectors with superior performance. Under the influence of concrete shrinkage, the longitudinal shear force on the joint surface of the composite bridge will increase. In addition, near the middle fulcrum, due to the large vertical shear force, the shear force of the joint surface in the local area is also large. Therefore, the beam end and the middle fulcrum should be strengthened against shear connectors. The strengthening range of the beam end should be less than 1/10 of the distance between the main beams and the span of the main beams.

In addition to confirming the factors affecting the shear strength of narrow-width steel box girders through indoor loading tests (as shown in Table 3), with the development of computer technology, using machine learning and probability statistics methods to predict the shear strength and seismic effect has gradually become an important research direction.

Tadesse G. Wakjira [64] adopted the interpretative machine learning (ML) method to obtain a prediction model of four damage states across ultra-high-performance concrete bridge columns based on the limit state of the drift ratio. The results showed that the axial load ratio and the aspect ratio were the main factors determining the drift ratio, and the higher the reinforcement grade, the smaller the vulnerability of ultra-high-performance concrete columns. However, the more serious the degree of damage is, the less influence the reinforcement grade has on the reinforcement effect.

Tadele [65] used the classification and regression tree (CART) and vulnerability analysis methods to reach a conclusion on the change of mechanical properties of reinforced concrete and its impact on the seismic design of reinforced concrete bridge columns. The results show that 0.12% of the tensile test data are lower than the minimum ASTM standard requirements, and the change in longitudinal steel yield strength significantly affects the seismic response of circular bridge columns.

Tadesse G. Wakjira [66] used a machine learning (ML) method to obtain a prediction model for the shear resistance of concrete beams reinforced by inorganic composite materials. The results showed that the Extreme Gradient enhancement (XGBoost) model was superior to the existing model in terms of accuracy, safety, and economy, and the resistance reduction factor was identified through reliability analysis. The target reliability indices were 3.5 and 4.0, respectively.

To date, the shear strength prediction based on experimental analysis, statistical analysis, and machine learning methods has been relatively comprehensive [67], but with the continuous development and improvement of narrow steel box girder structures, whether the relevant laws are applicable to new structures still needs to be reviewed and confirmed.

Table 3. Test of the influencing factors on the shear resistance of composite beams.

References	Box Girder Concrete Filling Height/Box Girder Height	Box Girder Concrete Strength (MPa)	UHPC Wing/Wing Thickness	Loading Protocol	Comments
Zhu et al. [68]	0	n/a	1	The formal loading starts at 0. Before the loading force reaches 500 kN, force-controlled loading is adopted, with 25 kN per stage.	The tribute of UHPC fins against the shear capacity is about 50%, and the bridge function of UHPC fin–steel fiber is good.
Chen et al. [69]	1	65	1	The formal loading starts at 0. Before the loading force reaches 500 kN, force-controlled loading is adopted, with 25 kN per stage. After the loading force reaches 500 kN, displacement-controlled loading is adopted.	The tribute of UHPC fins against the shear capacity is about 50%, and the bridge function of UHPC fin–steel fiber is good. Effectively reduce wing cracking
Xue et al. [70]	1	44.3	0	Through force-controlled loading, the preload is 20, 40, and 60 kN.	Two continuous composite beam specimens were studied, and the results show that the double combination can inhibit the crack development of the concrete wing slab during the loading stage.
Liu et al. [71]	1		0 0.1	Monotonic static loading	The shear-bearing capacity of the steel–composite beam under negative bending moments is borne by the steel beam and concrete wing slab.
Al-Osta [72]	1	54	n/a	The loading process is divided into three stages: preloading, force-controlled loading, and displacement-controlled loading.	A formula for calculating the shear strength of UHPC–NC (Normal Concrete) composite beams was obtained. The method can effectively reflect the influence of various parameters such as the UHPC layer, reinforcement of the UHPC layer, and the size effect on the shear capacity of UHPC–NC composite beams.
Hussein [61]	1	52	n/a	Force control	Both the bonding UHPC prefabricated slab and the cast-in-place gouge UHPC layer can effectively improve the bearing capacity of the composite structure, but the cast-in-place gouge casting method is superior to the bonding of the prefabricated slab.

4. Progress of the Rapid Construction Technology of the Narrow-Width Steel Box–UHPC Composite Beam after a Disaster

The narrow steel box composite beam enhances flange plate thickness by reducing the box chamber width, thus minimizing the number of longitudinal stiffeners in the top and bottom plates and eliminating the need for transverse stiffener plates. This design approach streamlines bridge components by increasing the panel span and eschewing small longitudinal girders in favor of durable steel–concrete or prestressed concrete bridge panels [73,74]. Reduced components, particularly within the box, facilitate manufacturing, while the lightweight steel main beam enables easy transportation and installation. This configuration ensures optimal force distribution, strong curve adaptability, and alignment with the green road ethos of factorization, standardization, and mechanization. Consequently, the narrow-width steel box composite beam has gained traction internationally, notably in Japan. However, its adoption remains limited in other regions, where it is still in an exploratory phase. Thus, this chapter examines recent advancements through two exemplary cases and explores progress in construction technology for double-narrow and three-narrow steel box girders, while also contemplating prospects for innovative narrow steel box girder composite structures.

4.1. Double-Narrow Steel Box Girder

Take the 37 m + 3 × 50 m + 37 m continuous double-narrow steel box–concrete girder bridge in a mountain area of Sichuan Province, China as an example. There are many mountains in this area [75], and the geological environment is complex and prone to strong geological activities, such as earthquakes, landslides, collapse, etc. Traditional large bridge prefabrication equipment is difficult to deploy quickly. According to the site environment and the needs of bridge design and use, the project uses the double-narrow steel box girder combined with the jacking method for rapid construction. The jacking method [76–78] was developed in the construction of prestressed concrete beam bridges, characterized by simple equipment and fast construction speed, and is very suitable for the rapid reconstruction of bridges after a disaster. The fixed thrust method combined with narrow-width steel box–UHPC composite beams can be used to reconstruct bridges quickly in a poor construction environment after an earthquake. As shown in Figure 13, when using the jacking method to carry out the rapid construction of narrow steel box beams, it can be pushed from one side of a river or valley to the other side as long as the transportation conditions on one side are met [76,77,79]. To reduce the reaction of the fulcrum of the pier on the general section of the steel box, the steel box and the bridge panel of the double-narrow steel box–concrete composite bridge are pushed successively.

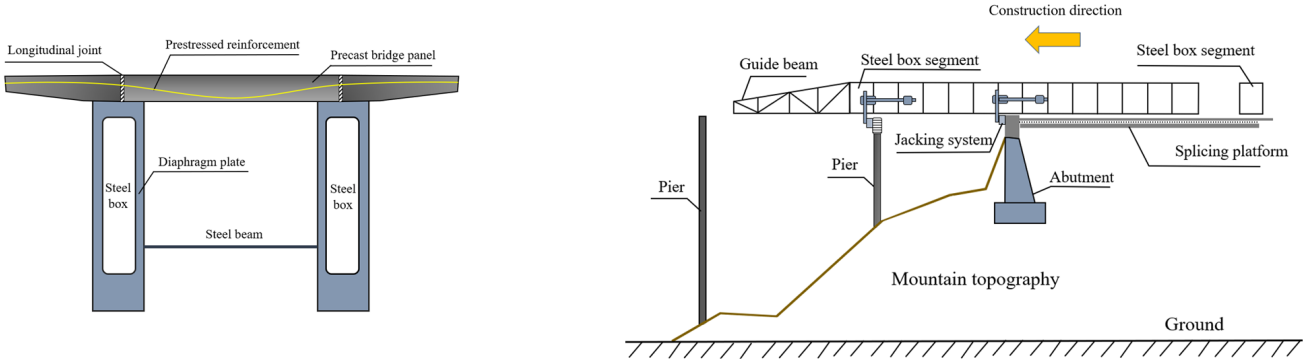

Figure 13. Rapid construction of a double-narrow steel box girder by the pushing method.

Under the specified viewing conditions, a platform is erected behind the abutment, or a steel box girder is positioned at the initial span. The multi-section steel box segments are interconnected and welded to create a unified steel box structure. Subsequently, sliding facilities for the steel box girder are installed. A pair of small-tonnage horizontal jacks are placed on each pier, with the pushing force being distributed across multiple points on the pier. Before the commencement of construction, careful examination of the pushing method's construction process is conducted, with particular attention paid to the localized stress on the steel box segment through the pier top. If deemed necessary, adjustments to the box's stiffener design can be made accordingly. A leading beam is installed during the pushing operation, with its length being 0.7 times that of the main span. Refer to the accompanying Figure 13 for visual representation. The analysis indicates that no intermediate temporary pier is required for spans of 50 m using this jacking scheme. Once the steel box is in position, prefabricated bridge panels are assembled on the splicing platform. Transverse prestress from the tensioned plates is applied to the box, after which the splicing platform is cleared for the installation of the next bridge panel section. This process is then repeated, as depicted in Figure 13. Similar procedures can be adopted for bridges to minimize the pushing distance. Connectors are installed at designated holes in the bridge panel after the full beam has been pushed into place. Welded bolts of perforated steel plate connectors may be welded or bolted as required.

The jacking method for double-narrow steel box–concrete composite beam bridges overcomes site, machinery, and concrete waiting constraints, significantly improving construction progress. It shortened the construction period by about 30%, crucial for rapid post-disaster reconstruction.

4.2. Three-Narrow Steel Box Girder

With advancements in design technology and concepts, narrow-width steel box girders have found application in the construction of long-span continuous beam bridges. Furthermore, the interface design of narrow-width steel box girders has evolved to introduce a novel form known as the three-narrow steel box girder. Illustrated by the case of a continuous three-narrow steel box composite girder bridge on an expressway in Zhejiang Province, China, spanning (50 + 85 + 50) m, the project mandates a short construction duration and uninterrupted traffic flow during execution. Hence, the construction plan involves the deployment of (50 + 85 + 50) m narrow-width steel box composite beams crossing the existing roadway in a left and right cross-hole layout, augmented by large-section lifting + bracket assembly. Narrow-width steel box composite beams can be flexibly arranged to accommodate various bridge widths. However, to fully exploit their structural advantages, main beam spacing should ideally be maximized. Employing steel composite bridge panels aids in reducing the weight of the bridge panel. Typically, the span of steel composite bridge panels does not exceed 6 m, with the overhang length limited to 0.4 times the span of the bridge panel between the main beams. Additionally, to meet the requirement of an 85 m span, the project introduces an innovative three-narrow steel box girder structure.

The web spacing of the steel box beam determines its width and distinguishes it from conventional steel box composite beams. For narrow steel box girders, the minimum web spacing should be at least 1.2 m to meet operational requirements. However, wider boxes require more steel. Due to the large span of the bridge and complexities in support stiffening and beam-to-roof positioning, the web spacing for the narrow steel box girder is set at 1.4 m, as shown in Figure 14.

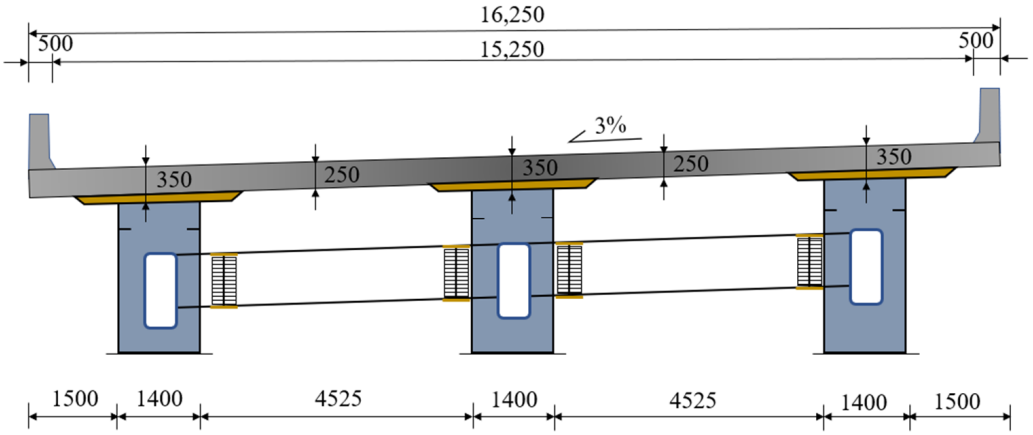

Figure 14. Three-narrow steel box girder section form.

4.3. Anti-Crack Control Measures of the Negative Bending Moment of the Fulcrum in the Narrow-Width Steel Box Continuous Beam with a Long Span

The bridge panel in the negative bending moment region at the fulcrum of a long-span continuous steel–concrete composite beam is susceptible to cracking. Common anti-cracking methods comprise prestressing, fulcrum forced displacement, ultra-high-performance concrete, weight compression, flexible connection, and construction procedure adjustment methods [75,80–84]. The prestressing method influences the internal forces [82,85] of the steel beam and entails a complex process. In practical applications, the flexible connection assembly method, represented by anti-pull and non-shear force nails, is typically employed in medium- and small-span composite beams measuring less than 60 m. Regarding the application of prestress and forced [86] displacement, the prestress effect diminishes [87] over time.

The compression method for large-span continuous steel–concrete composite beams is both costly and complex to implement. The forced displacement method necessitates substantial displacements of lifting and lowering beams. Utilizing ultra-high-performance concrete incurs higher costs. Based on calculations and practical experience with bridge construction, the method of adjusting the construction sequence is implemented for large-span continuous steel–concrete composite beams. Initially, concrete is poured in the positive bending moment zone of the bridge panel, followed by the pouring of concrete in the negative bending moment zone (within 0.15 times the span range around the central fulcrum). This approach does not significantly increase costs or complexity and facilitates convenient construction. This approach effectively controls the stress levels and crack widths in the bridge panel's negative bending moment region at the central fulcrum, meeting usage requirements comprehensively.

Section 4.2 uses the three-narrow steel box girder project in Zhejiang, China as an example. Prestressed UHPC wing slabs are used to control shear cracking in the negative bending moment area of the middle support, effectively reducing cracking and meeting stress and displacement requirements, as shown in Figure 15.

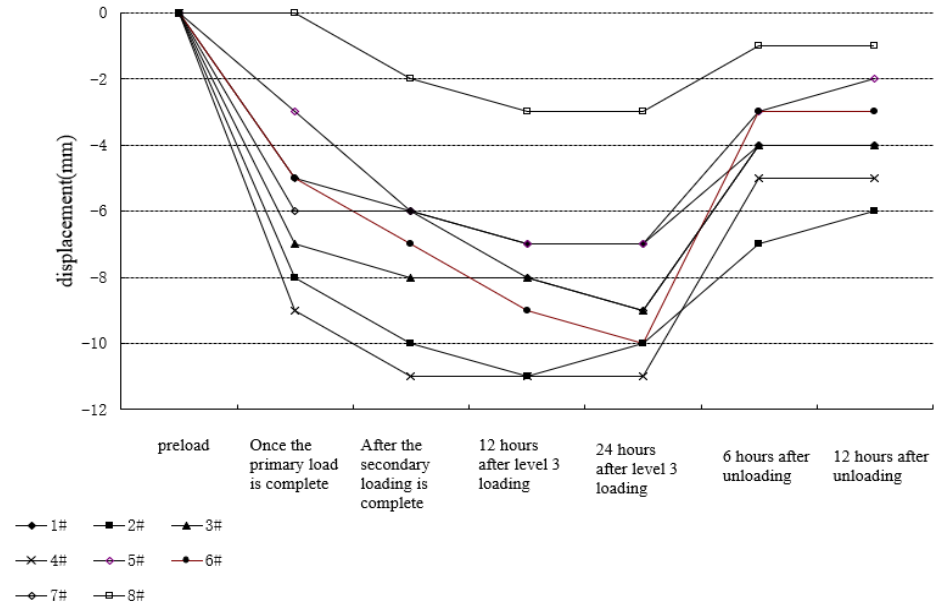

Figure 15. Test result of the precompression test in the negative bending moment area of the center fulcrum.

4.4. Narrow-Width Steel Box Girder Application Scenarios

The narrow steel box composite beam is a type of steel box composite beam. Considering the economic span of 45–75 m and the typical span of 60–100 m, it is important to maintain rationality in terms of processing, transportation, and structural forces. When the span exceeds 100 m, the height of the steel main beam needs to be above 4.2 m and divided during transportation. This compromises the advantages of convenient processing, transportation, and connection offered by narrow steel box girders, contradicting the design concept. Therefore, it is recommended that the maximum common span for narrow steel box composite girder bridges does not exceed 100 m.

(1) Small-radius flat-curved bridge or widened-ramp bridge in an interworking area with a span of 30 m or more

Curved bridges in the expressway interconnection face certain challenges, including cracking in reinforced concrete cast-in-place box girders and adaptability issues with prestressed concrete cast-in-place box girders. Furthermore, these curved bridges are often located beyond the height change point, resulting in possible lateral tilt changes for each span. Dealing with such situations using small box beams, T-beams, or short T-beams requires frequent adjustments to the steel mold and internal reinforcement arrangement of the prefabricated main beam, adding complexity to the construction process.

The narrow steel box girder adopts a closed steel box section, which has good torsional resistance and is more suitable for curved and inclined bridges. Compared to steel plate beams, it can adapt to the situation of curved bridges better. In addition, the narrow steel box composite beam box chamber is narrow, and with the bridge panel structure of a larger span, the transverse section layout is flexible, and it can also be applied to the greatly widened bridge.

According to the research of Ye Jianlong et al. [88], when span L $\leq$ 25 m, the small-radius flat-curved bridge can be better solved by the assembled structure of superimposed T-beams. In addition, when the span is less than 30 m, the construction of a narrow-width steel box composite beam is unreasonable and uneconomical. Based on this, it can be concluded that the narrow-width steel box composite girder bridge can conveniently solve the dilemma of the small-radius flat-curved bridge or the widened-ramp bridge in the interworking area with a span of 30 m or more, which has little choice of structure and strong applicability and competitiveness in this scenario.

(2) The main-line 60 ~ 100 m span of a mountain or an urban bridge

When the span of the main bridge is 60 m or less, more economical steel composite beams can be used for a more convenient span [89]. When the span is large, the continuous steel box composite beam structure is a more reasonable choice. The following table is a comparison of the material indicators of the narrow steel box composite beam bridge in the Kezhu Expressway project and the conventional slot steel composite beam bridge in other projects this year. It can be seen that compared to the conventional slot steel composite beam structure, the steel amount per unit area of the main beam, the steel amount of the whole bridge, and the painting area of the main beam of the narrow steel box composite beam within the span of 60~100 m have been improved by different degrees, saving about 15%, 4.3%, and 21% respectively, as shown in Table 4.

Table 4. Comparison of key indices between narrow steel box composite continuous beams and conventional steel-mixed composite continuous beams.

Item	① Conventional 85 m Main-Span Steel–Concrete Composite Beam	② Kezhu High-Speed 85 m Main-Span Narrow Steel Box Girder	③ Conventional 75 m Main-Span Steel–Concrete Composite Beam	④ Kezhu High-Speed 75 m Main-Span Narrow Steel Box Girder	②/①	④/③
Steel beam (kg/m^2)	457	397	411	339	0.869	0.825
Steel beam + bridge panel steel (kg/m^2)	584	562	521	496	0.962	0.952
coating (m^2/m^2)	9.28	7.28	9.33	7.32	0.784	0.785

5. Discussion and Design Suggestions

Considering only the contribution of the web to the shear strength, the calculated value of the shear strength will be much smaller. Whether it is the American AASHTO, the European code EC4, or the Chinese code GB 50917-2013, the calculated value of the shear strength is too small, which will greatly waste the design performance of the narrow steel box girder.

Based on the principle of superposition calculations of the shear capacity of each part, different scholars have carried out further research on the calculation formula of the shear force of narrow-width steel box girders, but there is still a complete and applicable calculation criterion for narrow-width steel box girders. Therefore, it is necessary to further review and study the calculation formula of the shear capacity of narrow-width steel box girders. At the same time, the main factors affecting the shear performance of the narrow steel box girder are UHPC steel fiber content, UHPC plate thickness, filling concrete, transverse partition in the box, interbeam, shear connector, etc. When designing a narrow-width steel box girder, it is necessary to design and verify the parameters of each influencing factor according to the field requirements. Finally, the rapid post-disaster construction technology of narrow-width steel box–UHPC composite beam is increasingly being developed. The new sectional structure and construction method can greatly improve the adaptability of narrow-width steel box girders under various engineering requirements and can also generate more new technologies and instruments to promote the development of the rapid post-disaster reconstruction technology of bridges.

6. Conclusions and Perspective

In this paper, the development of narrow steel box–UHPC composite beam structures, the influencing factors of the shear strength, and the predicted value of the shear strength under different specifications are reviewed, and the influencing factors of the shear strength

and the calculation method of the shear strength limit based on the superposition principle of the shear strength are summarized. The development of the rapid post-disaster construction technology of narrow-width steel box–UHPC composite beams in recent years is reviewed, and the new composite structure and post-disaster construction method of the narrow-width steel box are evaluated. Based on the above discussions, the following conclusions and recommendations can be derived:

1. Due to technological advancements in the use of high-strength materials and the increasing number of modern structures using concrete of high strength, some restrictions on narrow-width steel box–UHPC composite beams in the design specification need to be updated. In this paper, the Chinese code GB 50917-2013, the European code EC4, and the American code AASHTO are reviewed. The results show that the calculated values of the shear strength obtained by the above three codes are too conservative, and the predicted values of the shear strength obtained are less than 70% of the actual shear strength, resulting in a waste of shear strength. The calculation method of shear force based on the principle of superimposed shear capacity is not complete and lacks relatively complete and applicable calculation criteria.
2. According to the literature review, the main failures of UHPC composite beams under the condition of the negative moment zone are buckling deformation of the box girder, cracks on the upper surface of wing plates, and local concrete crushing. The main factors affecting the shear strength of the composite beam structure are shear span ratio, concrete wing plate, UHPC steel fiber content, UHPC plate thickness, and transverse partition in the box. The formula for calculating the shear capacity of a narrow-width steel box girder based on the superposition principle of shear capacity lacks a uniform conclusion regarding its applicability and needs further study.
3. The new double-narrow steel box girder structure and three-narrow steel box girder structure have a good application effect in the reconstruction of bridges after a disaster. For the long-span continuous beam bridge, the narrow steel box composite structure needs to use corresponding control measures to reduce the development of cracks at the middle support. At the same time, the scope of the application of the narrow-width steel box girder composite bridge is reviewed, and the conclusion is that the narrow-width steel box girder is mainly used in small-radius flat-curved bridges or widened-ramp bridges in interworking areas with a span of 30 m or more and in the main-line 60–100 m span in mountainous or urban areas.
4. The steel–concrete composite structure, with advantages in all aspects, has a wide range of applications in housing construction and large road and bridge construction. The construction method combined with narrow-width steel box–UHPC composite beams can be used to quickly rebuild bridges under poor construction environments after an earthquake, which is of great significance for post-disaster reconstruction projects.

Author Contributions: Conceptualization, Y.C.; Formal analysis and Writing—original draft, J.X.; Investigation, P.Y. and Q.W. and G.C.; Formal analysis, X.S. All authors have read and agreed to the published version of the manuscript.

Funding: The authors would like to acknowledge the financial support from the Innovation Capability Support Program of Shaanxi (Program No. 2023-CX-TD-35) and the Key Research and Development Program of Shaanxi (Program No. 2023KXJ-159).

Data Availability Statement: Not applicable.

Conflicts of Interest: Author Yunteng Chen was employed by the company Shaoxing Communications Investment Group Co., Ltd. Authors Peilong Yuan and Qiang Wang were employed by the company CCCC Second Highway Engineering Co., Ltd. The remaining authors declare that the research was conducted in the absence of any commercial or financial relationships that could be construed as a potential conflict of interest.

References

1. Meng, B.; Xiong, Y.P.; Zhong, W.H.; Duan, S.C.; Li, H. Progressive collapse behavior of composite substructure with large rectangular beam-web openings. *Eng. Struct.* **2023**, *295*, 116861. [CrossRef]
2. Gerasimidis, S.; Ellingwood, B. Twenty Years of Advances in Disproportionate Collapse Research and Best Practices since 9/11/2001. *J. Struct. Eng.* **2023**, *149*, 2. [CrossRef]
3. Fan, H.B.; Liu, T.; Zhang, S.Y.; He, H.J.; Zhu, Z.G.; Zhu, Y.Q.; Gao, X.Q. Effects of Jet-Grouting Piles on Loess Tunnel Foundation with Centrifugal Model Tests. *Int. J. Geomech.* **2023**, *23*, 3. [CrossRef]
4. Fang, Q.; Liu, X.; Zeng, K.H.; Zhang, X.D.; Zhou, M.Z.; Du, J.M. Centrifuge modeling of tunnelling below existing twin tunnels with different types of support. *Undergr. Space* **2022**, *7*, 1125. [CrossRef]
5. Jin, Z.X.; Zhang, C.P.; Li, W.; Tu, S.Q.; Wang, L.B.; Wang, S.X. Stability analysis for excavation in frictional soils based on upper bound method. *Comput. Geotech.* **2024**, *165*, 105916. [CrossRef]
6. Qiu, J.L.; Liu, Y.H.; Qian, X.Y.; Ma, C.; Liu, J.; Liu, T.; Han, H.X.; Ma, P.G. Guarantee rate statistics and product-moment correlation analysis of the optimal deformation allowance for loess tunnel in China. *Environ. Earth Sci.* **2024**, *in press*.
7. Li, Z.Q.; Lai, J.X.; Ren, Z.D.; Shi, Y.F.; Kong, X.G. Failure mechanical behaviors and prevention methods of shaft lining in China. *Eng. Fail. Anal.* **2023**, *143*, 106904. [CrossRef]
8. Qiu, J.L.; Liu, D.D.; Zhao, K.; Lai, J.X.; Wang, X.L.; Wang, Z.C.; Liu, T. Influence spatial behavior of surface cracks and prospects for prevention methods in shallow loess tunnels in China. *Tunn. Undergr. Space Technol.* **2024**, *143*, 105453. [CrossRef]
9. Tu, S.Q.; Li, W.; Zhang, C.P.; Chen, W. Effect of inclined layered soils on face stability in shield tunneling based on limit analysis. *Tunn. Undergr. Space Technol.* **2023**, *131*, 104773. [CrossRef]
10. Tu, S.Q.; Li, W.; Zhang, C.P.; Wang, L.B.; Jin, Z.X.; Wang, S.X. Seepage effect on progressive failure of shield tunnel face in granular soils by coupled continuum-discrete method. *Comput. Geotech.* **2024**, *166*, 106009. [CrossRef]
11. Wang, Z.C.; Cai, Y.C.; Xie, Y.L.; Zhang, M.Z.; Lai, J.X.; Qiu, J.L.; Liu, T. Laboratory study on mechanical behavior of hollow p-type steel-concrete composite support in loess tunnel. *Tunn. Undergr. Space Technol.* **2023**, *141*, 105280. [CrossRef]
12. Wu, K.; Zheng, X.M.; Zhao, N.N.; Shao, Z.S. Effect of compressible layer on time-dependent behavior of soft-rock large deformation tunnels revealed by mathematical analytical method. *Appl. Math. Model.* **2024**, *126*, 457. [CrossRef]
13. Xu, S.S.; Lai, J.X.; O'kelly, B.C.; Zhao, B.D. 3D deformation and strain fields in drying kaolinite obtained from tracking internal bubbles using X-ray CT and ANN. *Acta Geotech.* **2024**, *19*, 99. [CrossRef]
14. Xu, S.S.; Nowamooz, H.; Lai, J.X.; Liu, H.T. Mechanism, influencing factors and research methods for soil desiccation cracking: A review. *Eur. J. Environ. Civ. Eng.* **2023**, *27*, 3091. [CrossRef]
15. Yuan, P.L.; Zhang, B.D.; Yang, Y.T.; Jiang, T.F.; Li, J.; Qiu, J.L.; He, H.J. Application of polymer cement repair mortar in underground engineering: A review. *Case Stud. Constr. Mater.* **2023**, *19*, e02555. [CrossRef]
16. Zan, W.B.; Liu, L.J.; Lai, J.X.; Wang, E.B.; Zhou, Y.P.; Yang, Q. Deformation failure characteristics of weathered phyllite tunnel and variable-stiffness support countermeasures: A case study. *Eng. Fail. Anal.* **2023**, *153*, 107553. [CrossRef]
17. Liu, Y.H.; Qian, X.Y.; Qiu, J.L.; Chen, Y.H.; Liu, T.; Zhao, K.; Sun, H.; Liu, D.D. Disaster Analysis and Protection Measures of Coal and Gas Outburst for Coal Measures Strata Gas Tunnel in China. *KSCE J. Civ. Eng.* 2024; *in press*.
18. Zhao, Z.Z.; Sun, H.; Zhang, N.X.; Xing, T.H.; Cui, G.H.; Lai, J.X.; Liu, T.; Bai, Y.B.; He, H.J. Application of unmanned aerial vehicle tilt photography technology in geological hazard investigation in China. *Nat. Hazards* **2024**. [CrossRef]
19. Bekic, D.; Kerin, I.; Cahill, P.; Michalis, P.; Lapthorne, J.; Solman, H.; Gilja, G.; Potocki, K.; Pakrashi, V.; McKeogh, E. In BRIDGE SMS—INNOVATIVE SOLUTION FOR MANAGEMENT OF BRIDGES OVER WATER. In Proceedings of the 5th International Conference on Road and Rail Infrastructure (CETRA), Zadar, Croatia, 17–19 May 2018; pp. 57–63.
20. Niemierko, A. Modern bridge bearings and expansion joints for road bridges, 6th Transport Research Arena (TRA), Warsaw, Poland, April 18-21, 2016. *Transp. Res. Procedia* **2016**, *14*, 4040–4049. [CrossRef]
21. Tang, K.; Liu, D.; Xie, S.; Qiu, J.; Lai, J.; Liu, T.; Fang, Y. Analysis of loess water migration regularity and failure response of tunnel structure under rainfall environment. *Bull. Eng. Geol. Environ.* **2024**, *83*, 251. [CrossRef]
22. Zhang, Z.; Song, Z.; Lai, J.; Qiu, J.; Cheng, Y.; Zhang, J. Critical slowing down precursor information for the acoustic emission response characteristics of defective tuffs. *Theor. Appl. Fract. Mech.* **2024**, *129*, 104220. [CrossRef]
23. Li, Z.H.; Ma, E.L.; Lai, J.X.; Su, X.L. Tunnel deformation prediction during construction: An explainable hybrid model considering temporal and static factors. *Comput. Struct.* **2024**, *294*, 107276. [CrossRef]
24. Zan, W.B.; Lai, J.X.; Zhang, W.J.; Yang, Q.; Qin, Y.W.; Su, X.L. Experimental and applied research on similar materials to granular mixtures for the solid-liquid coupling model test of an underwater tunnel. *Constr. Build. Mater.* **2024**, *416*, 135170. [CrossRef]
25. Qin, Y.W.; Chen, Y.H.; Lai, J.X. Failures in Loess Slope-Tunnel System: An overview of trigging sources, acting mechanism and mitigation strategies. *Eng. Fail. Anal.* **2024**, *158*, 107996. [CrossRef]
26. Li, Z.; Lai, J.; Wang, M.; Qiu, J.; Zan, W. Collapse mechanism and treatments of a deep tunnel in the weathered granite fault zone. *Tunn. Undergr. Space Technol.* **2024**, *152*, 105891. [CrossRef]
27. Mao, M.; Yin, C.L.; Shen, S.Y.; Wan, Y. Experimental and Numerical Study on Flexural Behaviors of Steel-UHPC Composite Beams under Hogging Moment. *Ksce J. Civ. Eng.* **2024**, *28*, 2344–2354. [CrossRef]
28. Ataei, A.; Zeynalian, M.; Yazdi, Y. Cyclic behaviour of bolted shear connectors in steel-concrete composite beams. *Eng. Struct.* **2019**, *198*, 109455. [CrossRef]

29. Lu, X.Z.; Zhang, L.; Lin, K.Q.; Li, Y. Improvement to composite frame systems for seismic and progressive collapse resistance. *Eng. Struct.* **2019**, *186*, 227. [CrossRef]
30. Romero, M.L.; Espinós, A. Advances in Steel-Concrete Composite Structures (ASCCS 2018). *Structures* **2019**, *21*, 1. [CrossRef]
31. Zhang, Z.J.; Liu, Y.J.; Liu, J.; Xin, G.F.; Long, G.X.; Zhang, T.T. Experimental study and analysis for the long-term behavior of the steel-concrete composite girder bridge. *Structures* **2023**, *51*, 1305. [CrossRef]
32. Saiidi, M.; Douglas, B.; Feng, S. Prestress Force Efect on Vibration Frequency of Concrete Bridges. *J. Struct. Eng.* **1994**, *12*, 2233. [CrossRef]
33. Mcginnis, M.J.; Pessiki, S.; Turker, H. Application of Three-dimensional Digital Image Correlation to the Core—Drilling Method. *Soc. Exp. Mech.* **2005**, *4*, 359. [CrossRef]
34. Liu, S.; Wang, B.H.; Zheng, Y.; Mo, S.X.; Zhang, Q.Y.; Zhou, P.X. Experimental and Computational Research on the Shear Performance of Partially Filled Narrow-Width Steel Box-UHPC-Combined Girders under Negative Moment Action. *Buildings* **2023**, *13*, 2749. [CrossRef]
35. Wang, Y.C. Performance of steel-concrete composite structures in fire. *Prog. Struct. Eng. Mater.* **2005**, *7*, 86. [CrossRef]
36. Benedetty, C.A.; Santos, V.B.D.; Krahl, P.A.; Rossi, A.; de Andrade Silva, F.; Cardoso, D.C.T.; Martins, C.H. Flexural and shear behavior of steel-UHPC composite beams: A review. *Eng. Struct.* **2023**, *293*, 116649. [CrossRef]
37. Mo, S.; Xiong, H.; Zheng, Y.; Chai, L. Experimental study on shear strength of partially filled narrow steel box-UHPC composite beam. *J. Henan Polytech. Univ. (Nat. Sci.)* **2023**, *43*, 157–164.
38. Chen, H.; Nie, X.; Gan, S.; Zhao, Y.; Qiu, H. Interfacial imperfection detection for steel-concrete composite structures using NDT techniques: A state-of-the-art review. *Eng. Struct.* **2021**, *245*, 112778. [CrossRef]
39. Wakjira, T.G.; Alam, M.S. Peak and ultimate stress-strain model of confined ultra-high-performance concrete (UHPC) using hybrid machine learning model with conditional tabular generative adversarial network. *Appl. Soft Comput.* **2024**, *154*, 111353. [CrossRef]
40. Solhmirzaei, R.; Salehi, H.; Kodur, V.; Naser, M.Z. Machine learning framework for predicting failure mode and shear capacity of ultra high performance concrete beams. *Eng. Struct.* **2020**, *224*, 111221. [CrossRef]
41. Wakjira, T.G.; Abushanab, A.; Alam, M.S. Hybrid machine learning model and predictive equations for compressive stress-strain constitutive modelling of confined ultra-high-performance concrete (UHPC) with normal-strength steel and high-strength steel spirals. *Eng. Struct.* **2024**, *304*, 117633. [CrossRef]
42. Wakjira, T.G.; Kutty, A.A.; Alam, M.S. A novel framework for developing environmentally sustainable and cost-effective ultra-high-performance concrete (UHPC) using advanced machine learning and multi-objective optimization techniques. *Constr. Build. Mater.* **2024**, *416*, 135114. [CrossRef]
43. Chung, L.; Lim, J.-J.; Hwang, H.-J.; Eom, T.-S. Review of Design Flexural Strengths of Steel-Concrete Composite Beams for Building Structures. *Int. J. Concr. Struct. Mater.* **2016**, *10*, S109. [CrossRef]
44. Liu, J.; Liu, J.; Han, F.; Zheng, X. Research progress and application of coarse aggregate ultra high performance concrete used for lightweight steel-concrete composite structure. *J. Build. Struct.* **2022**, *43*, 36.
45. Nie, J.; Wang, J.; Gou, S.; Zhu, Y.; Fan, J. Technological development and engineering applications of novel steel-concrete composite structures. *Front. Struct. Civ. Eng.* **2019**, *13*, 1–14. [CrossRef]
46. Ranzi, G.; Leoni, G.; Zandonini, R. State of the art on the time-dependent behaviour of composite steel-concrete structures. *J. Constr. Steel Res.* **2013**, *80*, 252. [CrossRef]
47. Hao, X. Study of Shear Resistance of Partially Filled Narrow Steel Box-UHPC Composite Beam. Master's Thesis, Guilin University of Technology, Guilin, China, 2023.
48. Liu, X. Research on Bending Behavior of Narrow-Width Steel Box-UHPC Composite Beams Under Negative Moment. Master's Thesis, Guilin University of Technology, Guilin, China, 2023.
49. Luo, M.; Lin, P.; Yang, Z. Flexural Capacity of UHPC Reinforced Ordinary Concrete Composite Beam. *China Railw. Sci.* **2021**, *21*, 110722.
50. Yoo, S.W.; Choo, J.F. Evaluation of the flexural behavior of composite beam with inverted-T steel girder and steel fiber reinforced ultra high performance concrete slab. *Eng. Struct.* **2016**, *118*, 1–15. [CrossRef]
51. He, J.; Chao, L. Numerical analysis on shear resistance of ultra-high performance concrete-normal strength concrete composite beam. *Struct. Concr.* **2021**, *22*, 1128. [CrossRef]
52. Zhao, Q.; Xiao, F.; Zhang, H.; Fang, X.M. Behavior and reasonable design of steel-UHPC composite beams under negative moment. *J. Constr. Steel Res.* **2024**, *212*, 108268. [CrossRef]
53. Lu, W.L.; Peng, W.Q.; Zhu, L.; Ma, B.; Li, F.L. Study on mechanical behavior of steel-UHPC-NC composite beams under negative bending moment. *Case Stud. Constr. Mater.* **2022**, *17*, e01593. [CrossRef]
54. Yang, H. Finite Element Analysis of UHPC Flange-Narrow Width Steel Box Continuous Composite Beam's Double Combination Effects. Master's Thesis, Guilin University of Technology, Guilin, China, 2021.
55. Wang, Y. Experimental Study on Shear Strength of Concrete-Partial-Filled Steel Box Composite Continuous Beam under Negative Moment. Master's Thesis, Guilin University of Technology, Guilin, China, 2018.
56. Zhang, P.; Xu, F.; Liu, Y.; Sheikh, S.A. Shear behaviour of composite beams with permanent UHPC formwork and high-strength steel rebar. *Constr. Build. Mater.* **2022**, *352*, 128951. [CrossRef]

57. Chen, B.C.; Liu, A.R.; Zhang, J.P.; Zhang, F.; Bradford, M.A. Behavior of T-shaped embedded-nut bolted shear connectors in prefabricated steel-concrete composite beams. *Eng. Struct.* **2022**, *272*, 114983. [CrossRef]
58. American Association of State Highway and Transportation Officials. *AASHTO LRFD Bridge Design Specifications*; American Association of State Highway and Transportation Officials: Washington, DC, USA, 2017.
59. *EN 1994-2*; London Eurocode 4: Design of Composite Steel and Concrete Structures Part 2: General Rules and Rules for Bridges. British Standards Institution: London, UK, 2005.
60. *GB 50917-2013*; Code for Design of Steel-Concrete. Composite Bridges China Planning Publishing House: Beijing, China, 2013.
61. Hussein, L.; Amleh, L. Structural behavior of ultra-high performance fiber reinforced concrete-normal strength concrete or high strength concrete composite members. *Constr. Build. Mater.* **2015**, *93*, 1105. [CrossRef]
62. Men, P. Study on Shear Performance and Shear Capacity Calculation Method of Steel-Concrete Composite Girders in Negative Moment Regions. Ph.D. Thesis, Chongqing University, Chongqing, China, 2021.
63. Shozo, N. Study on Fatigue Design Load for Steel Bridge Piers and Steel Girder Bridges; Kaken. 2005. Available online: https://kaken.nii.ac.jp/en/grant/KAKENHI-PROJECT-17560429/ (accessed on 27 April 2024).
64. Wakjira, T.G.; Alam, M.S. Performance-based seismic design of Ultra-High-Performance Concrete UHPC) bridge columns with design example–Powered by explainable achine learning model. *Eng. Struct.* **2024**, *214*, 118346. [CrossRef]
65. Tadele, S.; Aldabagh, S.; Zhang, Q.; Alam, M.S. Variability of mechanical properties of steel rebars in North America and its effects on the seismic fragility of reinforced concrete columns. *Eng. Struct.* **2023**, *295*, 116805. [CrossRef]
66. Wakjira, T.G.; Ebead, U.; Alam, M.S. Machine learning-based shear capacity prediction and reliability analysis of shear-critical RC beams strengthened with inorganic composites. *Case Stud. Constr. Mater.* **2022**, *16*, e01008. [CrossRef]
67. Niu, F.; Liu, Y.; Xue, F.; Sun, H.; Liu, T.; He, H.; Kong, X.; Chen, Y.; Liao, H. Ultra-high performance concrete: A review of its material properties and usage in shield tunnel segment. *Case Stud. Constr. Mater.* 2024; *in press*.
68. Zhu, J.S.; Wang, Y.G.; Guo, X.Y. Experimental study on shear behaviors of steel-UHPC waffle plate composite beams. *China J. Highw. Transp.* **2020**, *33*, 11.
69. Chen, X.; Su, Q.; Chong, W. Experimental study on double composite action in the negative flexural region of two-span continuous composite box girder. *J. Constr. Steel Res.* **2011**, *67*, 10.
70. Xue, J.Y.; Cheng, G.; Zhao, H.T. Experimental study on shear performance of steel-concrete compositebeams under negative bending moment. *J. Build. Struct.* **2008**, *4* (Suppl. S1), 29.
71. Liu, C.; Ji, H. Shear resistance of ultra-high performance concrete-concrete composite beams. *J. Tongji Univ. Sci.* **2019**, *47*, 7.
72. Al-Osta, M.A.; Isa, M.N.; Baluch, M.H.; Rahman, M.K. Flexural behavior of reinforced concrete beams strengthened with ultra-high performance fiber reinforced concrete. *Constr. Build. Mater.* **2017**, *134*, 279. [CrossRef]
73. Chen, N.; Liu, L.; Deng, M.; Yang, C.; He, J. Tendency prediction and prevention strategy of geohazards triggered by Lushan Ms 7 earthquake, Sichuan Province, China. *J. Chengdu Univ. Technol. Sci. Technol. Ed.* **2013**, *40*, 371.
74. Hua, W.; Xin-Hua, Z. Earthquake-damages of reservoirs in Sichuan Province and rehabilitation countermeasures after disaster. *Water Resour. Hydropower Eng.* **2009**, *40*, 16.
75. Xu, X.; Zheng, F.; Guan, Y.; Yao, Y.; Qin, C. Spatiotemporal Characteristics of Earthquake Disasters and Their Damages within 2013 in China. *Res. Soil Water Conserv.* **2015**, *22*, 321.
76. Li, J.; Zeng, Y.; Chen, H.; Liu, X.; Song, X.; Ma, K. Study on mid-span jacking force for long span continuous rigid-frame bridges. *J. Railw. Sci. Eng.* **2015**, *12*, 335.
77. Wei, X.; Wei, G. Study on calculational method of ground settlement induced by level parallel pipe jacking. *Rock Soil Mech.* **2006**, *27*, 1129.
78. Li, G.; Feng, X. Study on Jacking Technology for Closure of Long-span Hybrid Girder Cable-stayed Bridge at Low Temperature. *J. Highw. Transp. Res. Dev.* **2019**, *36*, 69.
79. Wu, J.D.; Li, N.; Hu, A.J.; Zhang, P.; Liu, X.Q.; Wen, Y.T. Indirect Economic Loss Estimation of Wenchuan Earthquake to Sichuan Province in China Based on the ARIO Model. In Proceedings of the International Disaster and Risk Conference, Chengdu, China, 13–15 July 2009.
80. Gao, H.S.; Li, B.C.; Jian, J.S.; Yu, T.T.; Liu, H.B. Integral jacking of concrete continuous box beam bridge. *Structures* **2023**, *54*, 1026. [CrossRef]
81. Wang, P.; Liu, X. Primary Technical Investigation on Double Narrow Steel Box Girder of Bridge Rebuilt after Earthquake. *Technol. Highw. Transpor.* **2008**, *12*, 5.
82. Takayuki, K. Study on the Design Method of Prestressed Reinforced Concrete Beams Subjected to Torsion; Kaken. 1989. Available online: https://kaken.nii.ac.jp/en/grant/KAKENHI-PROJECT-01550380/ (accessed on 27 April 2024).
83. Jia, X.; Ji, L.; Cao, C.; Chen, X.; Yu, F. Influence of fulcrum and load positions on springboard mechanics. *J. Tsinghua Univ. (Sci. Technol.)* **2004**, *44*, 201.
84. Gao, S.; Wang, L. Research on Simply-Supported Continuous Bridge's Internal Force Optimized by Unequal Altitude Bearings. *Appl. Mech. Mater.* **2012**, *178*, 2353–2356. [CrossRef]
85. Lu, Z.-F.; Liu, M.-Y. Long-time Prestress Losses Analysis Method for Concrete Structure. *J. Wuhan Univ. Technol.* **2011**, *33*, 83.
86. Hitoshi, S. Nonlinear Hysteresis Behavior of Precast/Prestressed Concrete Member; Kaken. 1996. Available online: https://kaken.nii.ac.jp/en/grant/KAKENHI-PROJECT-08455247/ (accessed on 27 April 2024).

87. Rational Maintenance Method of Prestressed Concrete Bridge Considering Stress Corrosion Cracking of Prestressing Steel Wires; Kaken. 2022. Available online: https://kaken.nii.ac.jp/en/grant/KAKENHI-PROJECT-22K04259/ (accessed on 27 April 2024).
88. Ye, J.L.; Hu, S.X.; Yu, M.F.; Guo, B.Q. Research on New Prestressed Concrete Superposed Bridge. *Technol. Highw. Transp.* **2020**, *36*, 67–75+83.
89. Shen, D.W.; Ji, B.H.; Sun, Q.; Yang, X.H.; Zheng, H.; Rui, F. Analysis and estimation of the cost of the whole synchronous jacking project of bridge. *Constr. Econ.* **2012**, *5*, 32–34.

Disclaimer/Publisher's Note: The statements, opinions and data contained in all publications are solely those of the individual author(s) and contributor(s) and not of MDPI and/or the editor(s). MDPI and/or the editor(s) disclaim responsibility for any injury to people or property resulting from any ideas, methods, instructions or products referred to in the content.